

## Spark Plasma Sintering Simulation of Alumina Composite Modified with Carbon Nanotubes

Natalia A. Fedosova, Eleonora M. Koltsova\*, Evgeniy V. Zharikov, Ivan I. Mitrichev, Anna S. Shaneva

Dmitry Mendeleev University of Chemical Technology of Russia, Miusskaya sq. 9, 125047 Moscow, Russia  
 kolts@muctr.ru

Ceramic alumina composites with carbon nanotubes (20 - 50 %vol.) were prepared by spark plasma sintering method. Dependence of the composite strength from porosity and the amount of CNTs was found. The process of spark plasma sintering was investigated to develop mathematical model of this process. Resulting model of sintering process can predict porosity of composite Al<sub>2</sub>O<sub>3</sub>-CNT after thermal exposure. Optimization of sintering parameters was allowed to find heating mode for obtain composite samples with porosity less than 0.1 %

### 1. Introduction

Ceramic materials are widely used as a basis for protective coatings, thermal insulation and construction materials. Often they are used for the production of machinery parts exposed high temperature and high mechanical loads. Creating ceramic composites is effective way to reduce the brittleness of ceramics. Type of toughening agent depends on the kind of ceramic matrix and desirable properties of the final composite material (Cho et al., 2009). Carbon nanotubes (CNT) and carbon nanofiber (CNF) are the most common and most effective reinforcing particles for ceramic matrixes (Ghobadi et al., 2014).

CNTs are carbon structures which have extraordinary properties (Kasperski et al., 2013). The ratio of length to diameter and high strength CNTs (1 TPa) can significantly improve the composite strength parameters. Reinforcement the ceramic matrix may be due to several toughening mechanisms such as crack deflection, fiber pull-out and crack bridging mechanism (Xia et al., 2004). Composite ceramic materials modified carbon nanotubes exhibit excellent mechanical properties and have a lower density than the unreinforced ceramics.

Spark plasma sintering (SPS) is the most modern and efficient technology consolidation of powder materials. It is based on the use of directional pulsed electric current at a low atmospheric pressure. High energy and low voltage pulsating current generate spark plasma at high local temperatures between particles (up to 10,000 °C) (Wang et al., 2004). This leads to instantaneous thermal and electrolyte diffusion. Use SPS technique can reduce the maximum temperature of heating the material at 200 - 500 °C while the sintering duration is reduced to several minutes. The high heating and cooling rates increase the density of the final composite structure (Riggs et al., 2000) and reduce the rate of grain growth of the ceramic matrix (Suarez Riggs et al., 2013).

The aim of this work is a computer simulation of the spark plasma sintering ceramic composite material reinforced by CNTs, optimization of sintering parameters in order to obtain composites with zero porosity and high strength characteristics.

### 2. Experimental investigations

Initial composite powder obtained from a commercial alumin (α-Al<sub>2</sub>O<sub>3</sub> – 99 %, a grain size of 3-4 μm) and CNT obtained by pyrolysis of mixture hydrogen and methane (Fedosova et al., 2014). Ultrasonic dispersing CNTs was carried out in an aqueous solution of polyvinyl alcohol (1 %) (Fedosova et al., 2015). The homogeneous distribution of nanotubes in the bulk alumina matrix provides intensive mixing suspension of CNTs and

alumina powder in a planetary mill. After drying composite suspension and pelleting of the composite powder was obtained composite powder  $\text{Al}_2\text{O}_3\text{-CNT}$  with 20-50 %vol. CNT. SPS of a composite powder  $\text{Al}_2\text{O}_3\text{-CNT}$  produced on installing HP D25 (FCT Systeme GmbH, Germany). Pressure load, atmosphere, heating rate, maximum temperature and time of thermal action were set using of the program software HP D25. During the SPS experiments heating rate was varied from 200 to 380 °C/min, the maximum sintering temperature ranged from 1,500 to 1,600 °C. Isothermal holding time at the maximum temperature and load were constant (3 minutes and 20 kN respectively). Table 1 shows the results of experimental work, SPS modes and properties of the ceramic matrix composites  $\text{Al}_2\text{O}_3\text{-CNT}$  (porosity, flexural strength, fracture toughness). Measurement of flexural strength was carried out on a tensile testing machine Istron 5581 (Istron, USA). The fracture toughness was evaluated by indentation of a diamond Vickers pyramid under load. A more detailed description of a series of experiments to obtain composite samples presented in (Yi et al., 2015) and (Inbaraj et al., 2012).

Table 1: Spark plasma sintering conditions and properties of composite samples.

CNT volume, %vol.	Heating rate, °C/min	Max temperature, °C	Flexural strength, MPa	Fracture toughness, $\text{MPa}\cdot\text{m}^{1/2}$	Porosity, %
50	350	1,500	580	5.9	3.05
50	367	1,550	640	6.9	0.26
50	383	1,600	630	7.2	0.20
30	200	1,500	250	4.5	10.33
30	200	1,550	470	5.1	3.21
30	200	1,600	550	6.9	< 0.1
20	300	1,500	390	4.6	5.78
20	300	1,550	430	4.8	2.12
20	300	1,600	520	6.2	< 0.1
0	300	1,500	380	2.4	6.98
0	367	1,550	410	2.9	0.11
0	200	1,600	430	3.5	< 0.1

The results of the studies of the properties of the ceramic composite  $\text{Al}_2\text{O}_3\text{-CNT}$  samples can be concluded that the strength characteristics are directly dependent on the amount of the CNT and porosity of composite material. By increasing the amount of CNT is observed a gradual increase of the flexural strength and fracture toughness. Conversely, increasing the porosity of the composite tends to reduce the strength characteristics. Consequently, to obtain a composite  $\text{Al}_2\text{O}_3\text{-CNT}$  is necessary to provide the absence of porosity after the spark plasma sintering composite powder. Below is a mathematical model describing the SPS process, which allows numerical experiments to identify the sintering parameters provide a final porosity of the composite material less than 0.1 % and a high value of flexural strength and fracture toughness, respectively.

### 3. Mathematical modeling and optimization

As a result of experiments, it was found that the strength of the composite depends on the porosity value. It allows us to use this characteristic as the basis of a mathematical model. In the process of developing a mathematical description of changes in composite compact porosity, we take into account physical parameters of the processes: heating rate, maximum temperature, holding time at the maximum temperature, CNTs volume and the current state of composite powder compact (current temperature and current size of pores).

To describe the process of porosity decrease during sintering we introduce function of pore size distribution  $f(t, l)$ , where  $t$  – time,  $l$  – pore diameter. This function shows the state of powder compact in moment  $t$ . The equation describing the process of decreasing pores is:

$$\frac{\partial f}{\partial t} - \frac{\partial f \eta(t, l)}{\partial l} = 0; \quad t \in [0; t_{max}]; \quad l \in [0; l_{max}] \quad (1)$$

$f(t, l)$  - function of the pore size distribution,  $t$  - process - time,  $\eta$  - speed pore size change speed overgrowing of pores,  $l$  - pore diameter.

For the first stage of sintering (heating stage) driving force reduction process depends on the heating rate  $\Delta T/\Delta t$ , current pore diameter  $l$ , current temperature  $T$  and the volume of CNTs  $V_{CNT}$ . For the second stage

driving force depends on the difference in maximum temperature and recrystallization temperature ( $T_{max} - T_{recr}$ ), current pore diameter  $l$  and the volume of CNTs  $V_{CNT}$ .

$$\eta_1 = k_1 \cdot \left( \frac{\Delta T}{\Delta t} \right)^{m_1}; \quad \begin{cases} k_1 = a_1 + b_1 \sqrt{l^3} + c_1 T \\ a_1 = a_{10} + b_{10} V_{CNT} + c_{10} V_{CNT}^2 \end{cases} \quad (2)$$

$$\eta_2 = k_2 \cdot (T_{max} - T_{recr})^{m_2}; \quad \begin{cases} k_2 = a_2 + b_2 \sqrt{l^3} \\ a_2 = a_{20} + b_{20} V_{CNT} + c_{20} V_{CNT}^2 \end{cases} \quad (3)$$

$\eta_1$  and  $\eta_2$  – the rate of decrease pore size on the 1st and 2nd stage of sintering;  $k_1$  and  $k_2$  - phenomenological coefficients considering dependence of the speed of pore size decrease from the CNTs volume  $V_{CNT}$  (parameters  $a_1$  and  $a_2$ ); the current size of the pores  $l$  and the current temperature in the sintering chamber  $T$ ;  $m_1$  and  $m_2$  – constants characterizing the degree of deviation of system from balance state for the 1st and 2nd stage of sintering.

Looking for solutions of differential equations are used schemes with different error value. Most of the schemes are numerically stable. This fact creates a restriction on the ratio of the time step and step in space used in the calculation. We have worked to developed absolutely numerical stable method for solving differential equations. The numerical errors of this new scheme are proportional to the square of the time step and the square of the space step. Figure 1 shows stencil of new differential scheme, we called "Z-scheme".

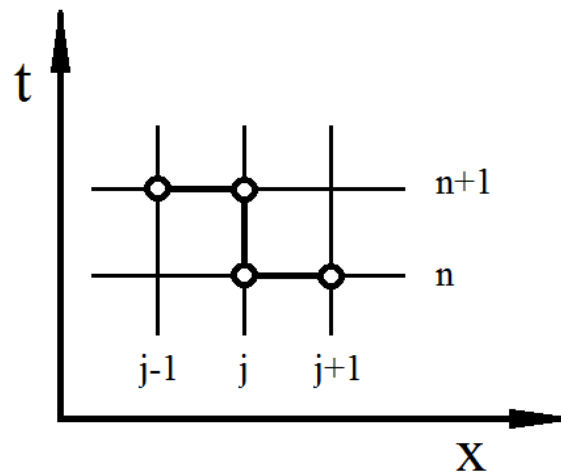


Figure 1: Stencil of new absolutely numerical stable "Z-scheme"

We used this new differential scheme "Z-scheme" to solve the Eq(1):

$$\frac{f_j^{n+1} - f_j^n}{\Delta t} - \frac{1}{2} \left( \frac{f_{j+1}^{n+1} \eta_{j+1}^{n+1} - f_j^{n+1} \eta_j^{n+1}}{\Delta l} + \frac{f_j^n \eta_j^n - f_{j-1}^n \eta_{j-1}^n}{\Delta l} \right) = 0 \quad (4)$$

$\Delta t$  – time step,  $\Delta l$  – a space step (pore size), index  $n$  is responsible for the time step, index  $j$  - per space step. Also we used in the initial condition and the right boundary condition:

$$f(t=0, l) = f^0(l); \quad f(t, l=l_{max}) = 0 \quad (5)$$

Initial pore size distribution  $f^0(l)$  is set according the law of normal distribution with pore diameter  $l$  from 0 to 5  $\mu\text{m}$  and a total porosity of 59 - 62 %. Right boundary condition corresponds to the absence of pores with maximum diameter ( $l_{max}$ ). Current porosity  $\varepsilon$  was calculated according to the formulas:

$$V_\varepsilon = \int_0^{l_{max}} \frac{4\pi}{3} \left( \frac{l}{2} \right)^3 f(l) dl; \quad \varepsilon = \frac{V_\varepsilon}{V_\varepsilon + V_{solid}} \cdot 100\% \quad (6)$$

$V_\varepsilon$  – total pore volume,  $V_{solid}$  – total solid volume,  $\varepsilon$  – porosity of the composite.

To determine the final form of the mathematical model, we carried out numerical search for values of the constants of the Eq(2)-(3). For this purpose was written a computer program which can be used to evaluate and specify the values of the kinetic parameters of the mathematical model. The search results are represented in Table 2. The search criteria are performed sum of the relative errors between the calculated and experimental porosity for each experiment:

$$S = \sum_{i=1}^N \left| \frac{\varepsilon_i^{\text{exp}} - \varepsilon_i^{\text{calc}}}{\varepsilon_i^{\text{exp}}} \right| \quad (7)$$

$S$  – criteria of optimization,  $\varepsilon^{\text{exp}}$  – experimental porosity value,  $\varepsilon^{\text{calc}}$  – calculated porosity value,  $N$  – number of experiments for constant search.

Table 2: Values of the constant of mathematical SPS model.

Constant of first sintering stage	Numeric value	Constant of second sintering stage	Numeric value
a <sub>10</sub>	$1.3 \times 10^{-3}$	a <sub>20</sub>	$5.2 \times 10^{-2}$
b <sub>10</sub>	$-5.7 \times 10^{-3}$	b <sub>20</sub>	$-3.6 \times 10^{-2}$
c <sub>10</sub>	$5.8 \times 10^{-3}$	c <sub>20</sub>	$2.5 \times 10^{-2}$
b <sub>1</sub>	$5.7 \times 10^{-3}$	b <sub>2</sub>	$16.1 \times 10^{-2}$
c <sub>1</sub>	$12.2 \times 10^{-3}$	m <sub>2</sub>	3.5
m <sub>1</sub>	1.7		

The adequacy of the resulting mathematical model was estimated according to the equation:

$$E_{\text{mod}} = \frac{1}{K} \sum_{i=1}^K \left| \frac{\varepsilon_i^{\text{exp}} - \varepsilon_i^{\text{calc}}}{\varepsilon_i^{\text{exp}}} \right| \cdot 100\% \quad (7)$$

$E_{\text{mod}}$  – total error of mathematical model,  $\varepsilon^{\text{exp}}$  – experimental porosity value,  $\varepsilon^{\text{calc}}$  – calculated porosity value,  $K$  – number of experiments for adequacy calculate.

The relative error  $E_{\text{mod}}$  of the resulting mathematical model accounted for 10.6 %.

The mathematical model Eq(1)-(3) is used to numerical experiments on SPS ceramic composite Al<sub>2</sub>O<sub>3</sub>-CNT (0-50 %vol.). Modeling used for calculating the current values of the function of the pore size distribution and current porosity of the composite material. Figure 2 and Figure 3 show results of numerical experiment for composite Al<sub>2</sub>O<sub>3</sub>-CNT (20 %vol.) which was sintered with heating rate of 300 °C/min and maximum temperature 1,600 °C.

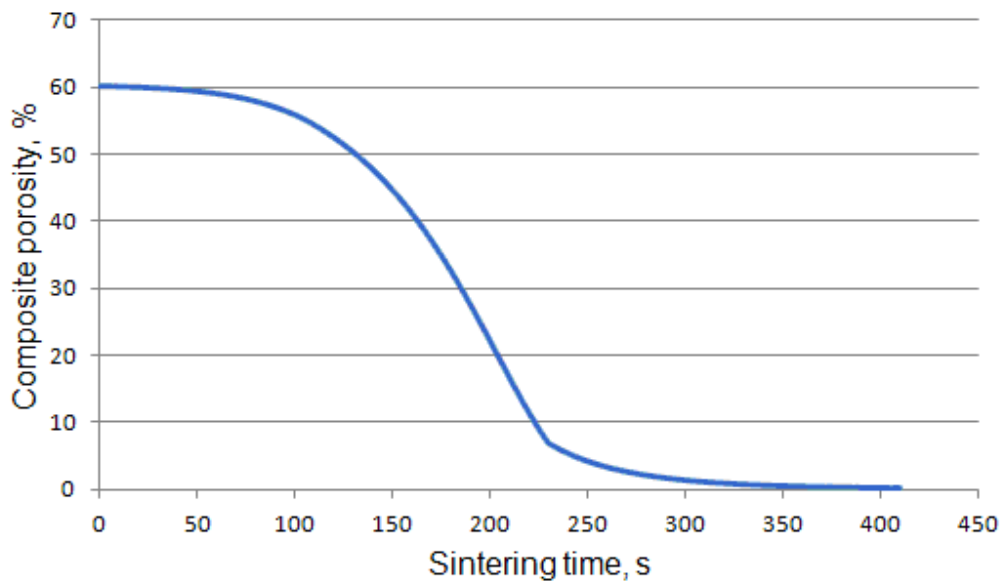


Figure 2: Porosity decrease in numerical experiment for composite Al<sub>2</sub>O<sub>3</sub>-CNT (20 %vol.).

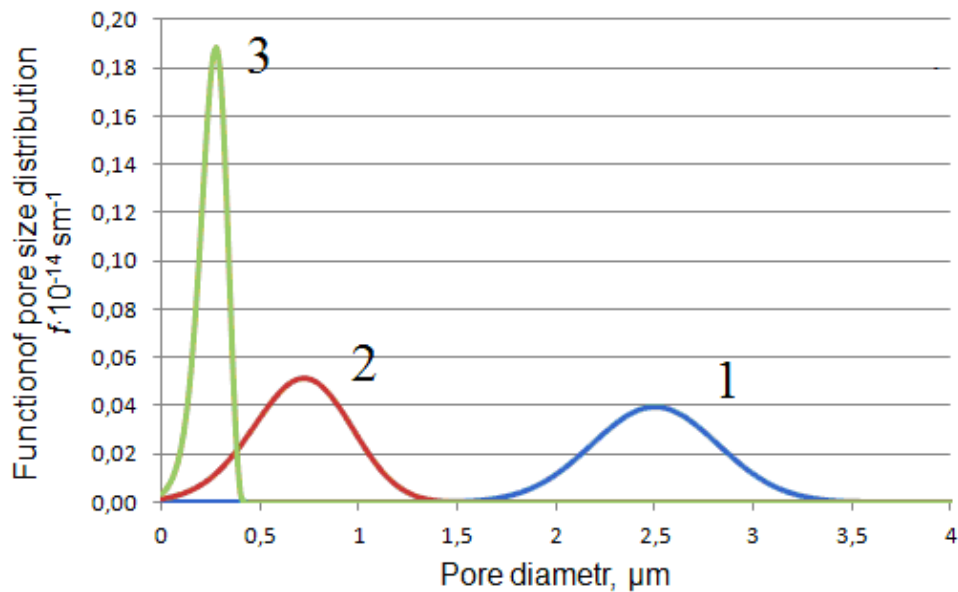


Figure 3: The results of numerical experiment for composite  $Al_2O_3$ -CNT (20 %vol.): function of pore sizes distribution: 1 – the initial distribution, 2 – distribution after the first sintering stage, 3 - distribution after the second sintering stage.

As the result of analysis of numerical experiments using a mathematical model SPS Eq(1)-(3), was found that the optimum temperature is 1,600 °C. It allows to reach the non-porous composite  $Al_2O_3$ -CNT (0 - 50 %vol.). Figure 4 shows the results of optimization of the CNT volume in composite powder with a sintering temperature of 1,600 °C and different heating rates: 200 °C/min, 300 °C/min, 383 °C/min. Increase in the volume fraction of CNTs increases the porosity of the composite, but the increase in the heating rate on the contrary decreases it. For receiving a non-porous  $Al_2O_3$ -CNT composite (porosity is less 0.1 %) at a heating rate of 383 °C/min CNT content should be less than about 30 %vol., for a heating rate of 300 °C/min – 20 %vol., the heating rate. 200 °C/min – 15 % vol.

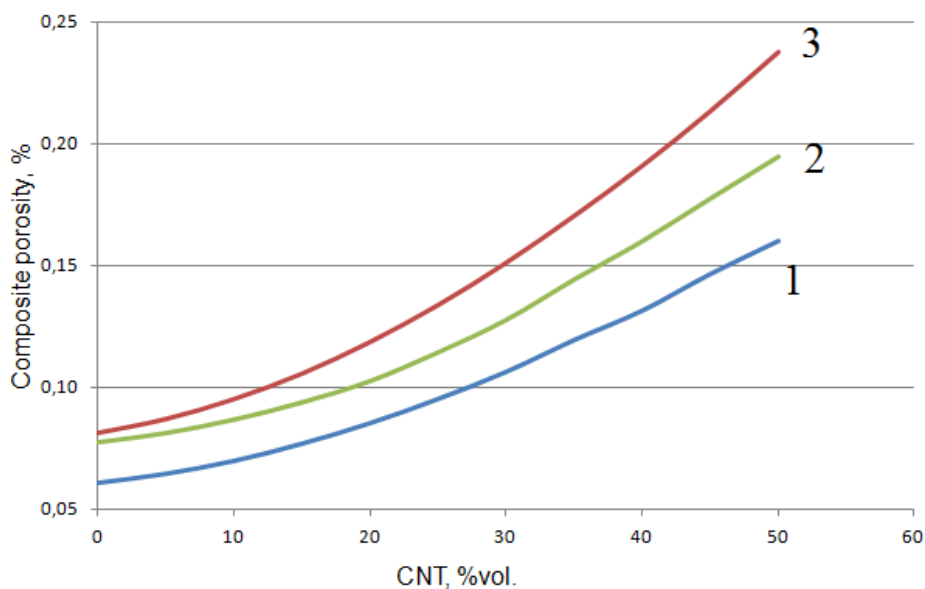


Figure 4: Porosity of the composite  $Al_2O_3$ -CNT at the differing heating rate and maximum temperature 1,600 °C. Heating rate: 1 – 383 °C/min, 2 – 300 °C/min, 3 – 200 °C/min.

#### 4. Conclusions

The mathematical model of spark plasma sintering ceramic composite Al<sub>2</sub>O<sub>3</sub>-CNT (20 - 50 %vol.) was developed. It is based on the equation of reduce composite powder porosity and is included the equations describing the heating stage by pulsed current and the stage of holding at the maximum temperature. Thermodynamic fluxes and driving forces of spark plasma sintering were identified and the differential equation describing the process was made up. The driving force of the first stage of the process the heating rate is defined. For the second stage it is the difference between the maximum temperature and the temperature of matrix recrystallization. The resulting equations include sintering parameters: the temperature, the current size of the pores and the amount of CNTs in the composite.

The authors developed the new differential scheme "Z-scheme". It is the absolutely numerical stable method of solving differential equations. The numerical errors are proportional to the square of the time step and the square of the space step. The pore size distribution and porosity value in each moment of the spark plasma sintering was calculated by "Z-scheme". Values of model constant parameters were calculated with an error of 10.6 %.

Computational experiments allowed to establish the dependence of the pore size distribution function and porosity of composite Al<sub>2</sub>O<sub>3</sub>-CNT with different volume of CNTs. It was found that to obtain a dense non-porous composite Al<sub>2</sub>O<sub>3</sub>-CNT (20-50 %vol.) necessary to carry out the SPS at 1,600°C. CNT volume must not exceed 30 %vol., 20 %vol. and 15 %vol. if the heating rate is 383 °C/min, 300 °C/min and 200 °C/min, respectively.

#### Acknowledgments

The work was supported by the Russian Science Foundation (RSF), project 14-19-00522.

#### Reference

- Cho J., Boccaccini A. R., Shaffer M. S., 2009, Ceramic matrix composites containing carbon nanotubes, *Journal of Materials Science*, 44(8), 1934-1951
- Fedosova N., Faikov P., Popova N., Koltsova E., Zharikov E., 2015, Ceramic Composite Material Obtained by Spark Plasma Sintering Technology with Carbon Nanotubes, *Glass and Ceramics*, 1(72), 13-16
- Fedosova N. A., Faikov P. P., Popova N. A., Duong T. T. T., Zaramenskikh K. S., Sovyk D. N., Zharikov E. V., 2014, Effect of the nature of carbon nanotubes on the structure and strength of ceramic composites, *Glass and Ceramics*, 71(3-4), 128-131
- Ghobadi H., Nemati A., Ebadzadeh T., Sadeghian Z., Barzegar-Bafrooei H., 2014, Improving CNT distribution and mechanical properties of MWCNT reinforced alumina matrix, *Materials Science and Engineering: A*, 617, 110-114, DOI: 10.1016/j.msea.2014.08.052
- Inbaraj S. R., Francis R. M., Jaya N. V., Kumar A., 2012, Processing and properties of sol gel derived alumina-carbon nano tube composites, *Ceramics International*, 38(5), 4065-4074.
- Kasperski A., Weibel A., Estournes C., Laurent C., Peigney A., 2013, Preparation-microstructure-property relationships in double-walled carbon nanotubes/alumina composites, *Carbon*, 53, 62-72.
- Riggs J.E., Walker D.B., Carroll D.L., Sun Y.P., 2000, Optical limiting properties of suspended and solubilized carbon nanotubes, *The Journal of Physical Chemistry B.*, 104(30), 7071-7076.
- Suarez M., Fernandez A., Kessel H. U., Hennicke J., Menéndez J. L., Kirchner R., Kessel T., 2013, Challenges and opportunities for spark plasma sintering: a key technology for a new generation of materials, INTECH Open Access Publisher.
- Wang X., Padture N. P., Tanaka H., 2004, Contact-damage-resistant ceramic/single-wall carbon nanotubes and ceramic/graphite composites, *Nature materials*, 3(8), 539-544
- Xia Z., Riester L., Curtin W. A., Li H., Sheldon B. W., Liang J., Xu J. M., 2004, Direct observation of toughening mechanisms in carbon nanotube ceramic matrix composites, *Acta Materialia*, 52(4), 931-944
- Yi J., Xue W.J., Xie Z.P., Chen J., Zhu L., 2015, A novel processing route to develop alumina matrix nanocomposites reinforced with multi-walled carbon nanotubes, *Materials Research Bulletin*, 64, 323-326